Arenal Deeps: application of numerical methods to 2D and 3D stability analyses of underground excavations

I. García Mendive, U. Sterin, G. Rellán & A. O. Sfriso
SRK Consulting Argentina SA, Buenos Aires, Argentina

M. Fuentealba
Orosur Mining Inc, Rivera, Uruguay

ABSTRACT: Arenal Deeps is an Au mine located near Minas de Corrales, Uruguay, which was exploited via an open pit operation from 2004 until 2009 and underground since then, using both inclined room and pillar and transversal stoping methods. The progression of mining activities (down to ~320m BGS) has led to an ever-growing complexity in the geometry of the mine, which cannot be adequately assessed solely with empirical design methods. This work presents a case study in which empirical and numerical methods were integrated to assess the stability of a stope roof and adjoining pillar. Empirical methods enabled straightforward determination of the need to include an intermediate pillar. A 3D boundary element model indicated that stress concentration in the roof was the main driver for instability. The 2D finite element model provided a FoS for roof failure of 1.20, considered adequate given the conservative plane-strain hypothesis it entails and geomechanical uncertainty.

1 INTRODUCTION

Arenal is a mesothermal epigenetic Au deposit located 400km North of Montevideo, Uruguay, hosted within basement amphibolite facies gneissic rocks inside the Proterozoic greenstone terrain known as the Isla Cristalina. (Golder 2009)

Mineralization is well constrained by upper (hangingwall) and lower (footwall) fault contacts within the 50-100m wide, east-west and northwest trending Rivera Shear zone. It has drill-defined dimensions of 900m along strike at surface and >700m down plunge, dipping moderately at 40-50 degrees to the south and steepening to more than 70 degrees at depth.

Structures are interpreted to be reverse faults and thrusts that predate the Rivera Shear. The main alteration assemblage associated with gold mineralization within the hosting structures comprises chlorite-(epidote)-carbonate-sericite-silica-pyrite.

The Arenal deposit was exploited via an open pit operation from 2004 until 2009. The final pit is ~500m long, 330m wide and 159m deep, having an inter-ramp angle of 47º–56º. The Arenal Deeps underground mine is a combination of six inclined room and pillar (IRP) sub-levels and seven transversal stoping (TS) sublevels, developed through a ramp that starts on the north wall of the pit, 98m below surface, and plunges 240m further below at a mean inclination of 8.5%.

Estimated mineral reserves are 276 kton for a cut-off grade of 2.53g/t Au for the IRP levels and 830 kton with cutoff grade of 3.25 g/t Au for the TS levels, totalling 1106 kton with 3.06 g/t Au cutoff grade. Adding the development reserves, probable mineral reserves add up to 1568 kton with cutoff grade of 2.87g/t Au. IRP operations extend from 150m to 250m below ground level and span roughly 1200m down dip and 180m along strike. Pillars are typically 5m high and 8m×8m across.

TS operations span depths of 200m to 350m below ground level and 180m along strike, divided into 25m-high sublevels. Stopes are typically 40m long and 20m wide; roof support consists of cable bolts installed on the access drifts, which are 5m×5m across and supported by split-sets and wire mesh. Primary and secondary stopes are filled with cemented rockfill and mine waste, respectively.

Continued exploitation of underground reserves has led to an ever-increasing complexity of excavation geometry for both the IRP and TS levels. The ore-body has proven to have grade that change abruptly in short distances, leading to the continuous finding of small new mineable bodies and occasionally to operational changes in size and shape of some stopes. This increased complexity of the mine, in turn, has fuelled the need for more involved stability assessments of stopes having thinner pillars and supporting side walls. Figure 1 shows an overall view of the underground mine.

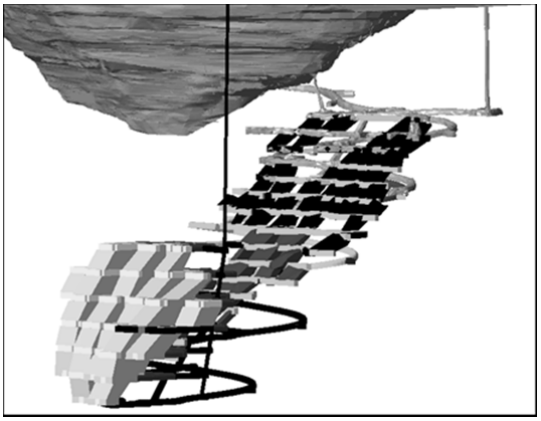

Figure 1. Overall view of Arenal and Arenal Deeps.

2 ANALYSIS METHODS

Both empirical and numerical methods for stope design and verification have been extensively employed in the operation. The former are based mainly on (Potvin 1988) chart, with the modifications proposed by (Villaescusa 2014). Empirical methods are very useful for the preliminary design of all stopes and for the final design of small, regular stopes that intersect only one geotechnical domain. However, they do not account for the complex mining-induced stress-field around stopes, nor do they provide a means of assessing safety or risk of local / general failure or spontaneous initiation of caving.

Numerical procedures properly account for much of the weakness of empirical methods at the cost of an involved analysis which is time-consuming, error-prone and data-demanding. The contour element method is a relatively straightforward numerical method that can yield the stress state around an opening of any shape with reasonable effort. Such stress-fields are a sound base case for the consistency check of the results of more sophisticated verifications. Being based on linear elasticity, this method still fails short in assessing risk or safety.

The finite element method addresses the shortcomings of the above methods, albeit at the cost of material parameter calibration, model setup, computing time and post-processing time. Advanced numerical codes available handle varied behaviour for multiple materials and involved geometries, and can account for the effect of construction sequence on stress-fields. A reasonably defined Factor of Safety can be computed for portions of the model, and estimates of risk can be therefore provided and supported by such analyses.

3 GEOTECHNICAL MODEL

3.1 *Geological model*

The Minas de Corrales Project is located within the Proterozoic greenstone/granite terrain known as the Isla Cristalina. Gold mineralization within the Isla Cristalina is spatially associated with the Rivera Shear, a regional east-west and northwest trending ductile/brittle-ductile shear zone that can be traced for approximately 110km along strike. Within this structural and geological pattern several mineral deposits have been recognized, the most important to date being San Gregorio, Santa Teresa and Arenal (Figure 2).

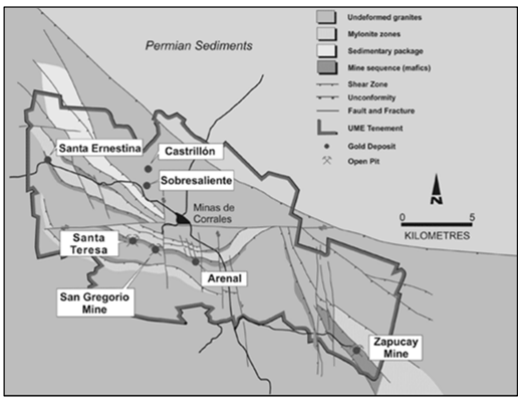

Figure 2. Regional geological map (Amec 2010).

The mineralized structures dip approximately 45° to the south at Arenal. These structures are interpreted to be reverse faults and thrusts that predate the Rivera Shear. The main alteration assemblage associated with gold mineralization within the hosting structures comprises chlorite-(epidote)-carbonate-sericite-silica-pyrite.

The mineralization of the Arenal "lode" has drill-defined dimensions of approximately 900m along strike at surface and >700m down dip/plunge. Arenal dips moderately at approximately 40-50 degrees to the south and steepening to greater than -70 degrees at depth.

Gold mineralization at Minas de Corrales is exclusively associated with epigenetic mesothermal style mineralization, consistent with the majority of Archaean and Proterozoic greenstone terrains worldwide.

Gold mineralization at the Arenal deposit occurs as infill of brittle fractures by silica-sulphide-gold bearing hydrothermal solutions. Brittle fracturing and brecciation occur within a wide shear zone with well-defined fault boundaries. Fracturing and brecciation are sealed with silicification with disseminated sulphide minerals and stock-work quartz-sulphide veining. High grade zones form plunging ore shoot geometry which is largely controlled by NW directed thrusting. Pyrite is the dominant sulphide mineral however minor galena and chalcopyrite have been observed. Gold occurrence is fine grained and visible gold is rare.

The Arenal deposit is hosted within basement amphibolite facies gneissic rocks. Lithologies present are quartz monzonites, monzonites and diorites.

3.2 *Structural model*

The Arenal deposit is hosted in east-west to northwest trending, low- to moderate-dipping thrust faults which define the San Gregorio Fault System (SGFS). It is constrained to the West and East by syn-mineral, NW-oriented, offsetting tear faults which followed and caused reactivation of the SGFS. The SGFS is fairly thoroughly mineralized, typically 50-100m wide, (Golder 2009) and well constrained by hangingwall (H1) footwall (F1) fault contacts.

H1, with a thickness of 1–2 m to 8–10 m, is the predominant shear zone that controls the hangingwall. It consists of monzonites with highly altered hydrothermal breccias, sericite, and carbonates of moderate strength (25MPa UCS). Local faults are ductile, intensely sheared, with clay fillings in the order of centimeters (Orosur 2010). Structural orientations for the hangingwall are 44/224, 13/270, 40/149 and 14/122 (Mello et al 2010).

F1 is the footwall shear zone that controls the orebody; it comprises highly-altered granites and diorites with sericite, chlorides and high-strength carbonates (80MPa UCS). Within the footwall, structures are mainly oriented at 20/130, 40/170 and 56/199.

The ore zone, composed mainly of granitic and monzonitic protoliths of ductile-brittle behaviour, is intensely and densely fractured (Orosur 2010). Discontinuities are generally closed. Main faults have attitudes of 230/47°, 268/37°, 187/52°, and 307/55°. Prominent discontinuities are oriented at 250/47, 108/27, 331/55, 129/79, and 029/86.

The principal geological elements of the Arenal deposit are shown in Figure 3.

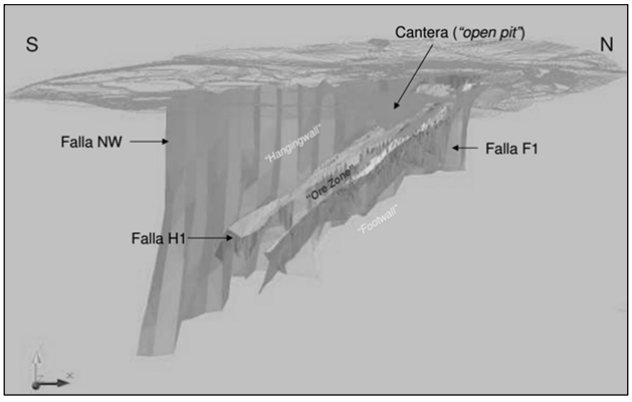

Figure 3. Major faults and orebody of the Arenal deposit (Amec 2010).

3.3 *Hydrogeological model*

The natural water level is high, close to the surface, as the pit is surrounded by a river and water bodies. However, due to the tightness of the structures and resulting low hydraulic conductivity of the rock mass (Iardino et al. 2010), infiltration is negligible throughout the underground operations. As a result, dry conditions can be assumed for the stability analyses of excavations.

3.4 *Geotechnical domains*

The rock mass quality was assessed according to the RMR_{76} CSIR classification system (Bieniawski 1976) at the intersections of the core drilling with two key operation areas: Inclined Room and Pillar (IRP) —named Ore Zone 1 (OZ1)— and Transversal Stoping —Ore Zone 2 (OZ2).

The lithological units found in the deposit were grouped into three domains:

- Hangingwall (HW): composed primarily of low- to moderately altered monzonites, including monzonite (MNZ), dyke trachyte (DYKT) and HW fracture zone (H1) units.
- Ore Zone (OZ): ore-bearing hydrothermal protoliths of granitic and monzonitic origin with sericitic/chloritic alteration and quartz and pyrite/carbonate veinlets. They comprise silicified breccia (OZB), carbonate (OZC), granite (OZG), monzonite (OZM) and mylonite (OZY) units.
- Footwall (FW): comprises granite (GRN) diorite (DIO) and fault zone (F1) units, with generally moderate to low degrees of alteration that include sericite, chlorite and carbonates.

HW, OZ and FW domains exhibit an average RQD of 80, 87 and 91%, respectively. Throughout the mine, Q averages 1.6 with a maximum of 8.6, whereas RMR76 averages 47 with a maximum of 63.

3.5 *Rock matrix*

Intact rock properties have been obtained through UCS (with/out strain measurements), triaxial compression and uniaxial tension tests, direct shear tests on discontinuities, point load tests and P- and S-wave tests.

The intact rock units (IRU) were grouped in the geotechnical domains HW, OZ or FW. The unit weight of the intact rock was on average 2.75kg/m^3. Within these units, the strongest rock is the FW granite, followed by diorite and mineral zones. The weaker units are the dyke trachyte and H1 zone. Within the mineral domain (OZ), the strongest rock is OZY and the weaker OZB. In general, the rocks constituting the HW domain are weaker than the FW rocks. A similar pattern arises in the OZ zone, where the mineral weakens as it approaches the HW.

For HW, OZ and FW, UCS average 27.0, 89.0 and 88.0 MPa and Young's moduli average 39.0, 73.0 and 51.0 Gpa, respectively. The main laboratory results are summarised in Table 1.

Table 1. Average properties of intact rock units.

IRU	Domain	Code	γ	UCS	E
[–]	[–]	[–]	[kg/m^3]	[MPa]	[GPa]
Monzonite	HW	MNZ	2.75	37.1	53.7
Trachyte dyke	HW	DYKT	2.71	19.2	–
Fault zone HW	HW	H1	2.73	24.5	24.1
Brecciated zone	OZ	OZB	2.81	41.0	95.3*
Carbonate Zone	OZ	OZC	2.84	80.0	55.2
Granite Zone	OZ	OZG	2.73	108.8	69.5
Monzonite Zone	OZ	OZM	2.70	73.9	82.7*
Mylonite Zone	OZ	OZY	2.77	139.3	63.3
Fault Zone FW	FW	F1	2.80	63.2	34.2
Granite	FW	GRN	2.63	100.1	69.8
Diorite	FW	DIO	2.79	99.5	49.9

* Values obtained from a single laboratory test.

4 NUMERICAL ANALYSES

An example of the design and stability analysis of an underground excavation is presented.

The stope is located 300m below ground level. The original geometry, taken as-is from the reserve estmation model, included an unsupported roof 62m×13-27m, and involved ~17.7kton at a grade of 2.15g/t, totalling 1344oz of metallic gold.

Analyses carried out via empirical (Potvin 1988) and contour element methods (Examine3D) indicated that roof stability could not be guaranteed.

Difficult accesss precluded the use of support elements; time constraints imposed by the production schedule ruled out the execution of borings to collect more detailed geotechnical data; the geotechnical model could not be refined in the vicinity of the excavation.

To account for the uncertainties and to reduce the operational risk of roof instability, a pillar 5.5m wide by 12m long was proposed. The pillar would reduce the span and lower the roof's hydraulic radius to acceptable levels, but at the cost of a reduction in recovery of ~148oz of gold. Owing to the complexity of the ensuing geometry, the design could not be studied by empirical methods but required the use of boundary element (Examine3D) and finite element methods (Phase^2).

4.1 *Geometry*

The final design, two stopes separated by a rib pillar, is shown in Figure 4. The geometry has an average height of 12 m, a maximum span of 62 m, and widths varying between 12.5 and 27.0m. The stopes are connected by an access drift having a 5.5m×5.5m cross-section, supported by 2.4m-long split-sets arranged in a staggered 1.30m×1.50m pattern. Figure 4 just shows the stope under analysis, omitting several other cavities that exist around and that significatively impact the stress field around the stope.

4.2 *Geotechnical model*

The generalized Hoek-Brown strength criterion (GHB) was employed for the rock mass (Hoek et al. 2002). A Poisson's ratio equal to 0.25 was considered. The Young's modulus was estimated considering Hoek & Diederichs (2006):

$$E_{rm}[\text{MPa}] = E_i[\text{MPa}] \cdot \left(0.02 + \frac{1 - D/2}{1 + e^{((60+15D-GSI)/11)}} \right) \quad (1)$$

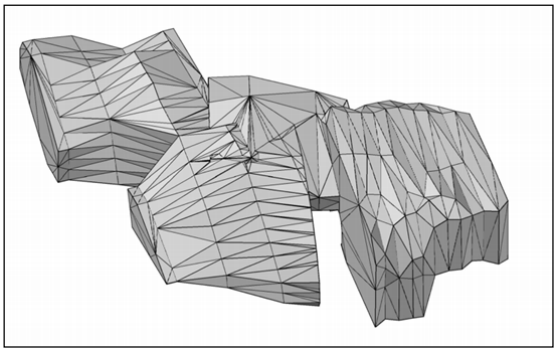

Figure 4. Geometry of IRP stopes and rib pillar.

Strength parameters (Table 2) were adopted on the basis of laboratory tests and in situ observations.

Table 2. Rock matrix and rock mass parameters.

Intact Rock			Rock mass					
E	UCS	m_i	GSI	E_{rm}	ν	γ	K1*	K2*
[GPa]	[MPa]	[–]	[–]	[GPa]	[–]	[kg/m^3]	[–]	[–]
67.5	90	10	50	20.0	0.25	2.7	1.5	1.2

* Stresses dir. K1 are oriented 15° dir. N-S and K2 105° E-W.

4.3 *Preliminary assessment*

The boundary element model suggested potential instability of the original geometry. The computed maximum induced stress parallel to the roof (σ_{max}=20 MPa) served as input for the chart estimation of stability using (Potvin 1988). Mapping records indicated an average value of Q = 2.74, Q = Q' since no water infiltration was observed and SRF = 1.

Structures that could have an effect on stability were interpreted from nearby cores and mappings; in the end, a structure with 45° dip was considered, whence the stability number yielded a value N' = 5.9.

Hydraulic radii —calculated for characteristic widths of 12.5m and 27.0m— were 5.2m and 9.4m, respectively. These parameters fall into the "stable with reinforcement" and "transition" zones in Potvin's chart. Additionally, an admissible hydraulic radius of HR_{max} = 6.8m was calculated by means of (Nickson 1992) expression.

Taking into account both geotechnical uncertainty and the limitations of the methods employed, unsupported roof stability could not be guaranteed.

4.4 *Subsequent numerical analyses*

The boundary element method was used to calculate the induced stress field. Stability of roof and pillar was assessed by means of the point utilization factor

$$\mathrm{FUP} = \frac{\sigma_1}{\sigma_{1\,\mathrm{GHB}}} \qquad (2)$$

where σ_1 is the maximum principal induced stress (elastic) and $\sigma_{1\,\mathrm{GHB}}$ is the corresponding strength according to GHB.

This factor indicates the amount of utilization in terms of stresses, but it does not provide an estimate of FoS or of the risk of failure.

Figure 5 and Figure 6 show maps of principal stress distribution maps for a longitudinal section perpendicular to the pillar axis.

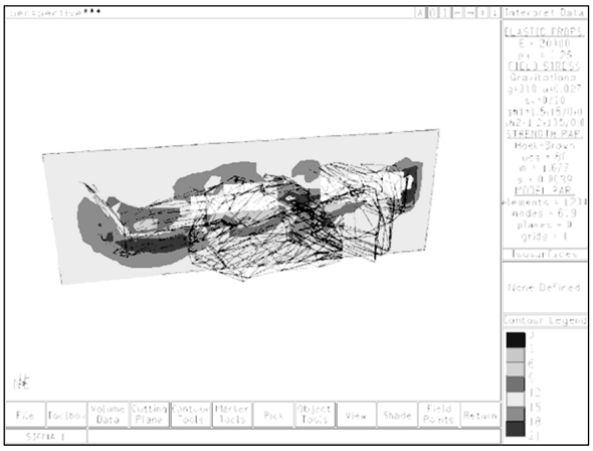

Figure 5. Map of major principal stress σ_1 (Examine3D).

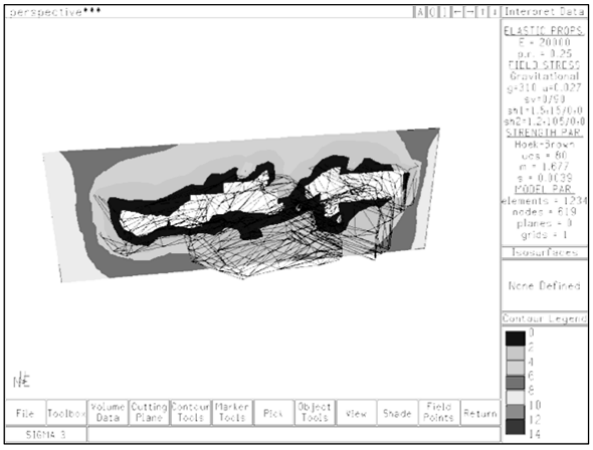

Figure 6. Map of minor principal stress σ_3 (Examine3D).

Figure 7 shows an isosurface for FUP = 1, i.e. $\sigma_1 > \sigma_{1\,\mathrm{GHB}}$ for points located between it and the stope roof. Although the surface does not represent a potential failure mechanism, it does suggest possible localized vaulting.

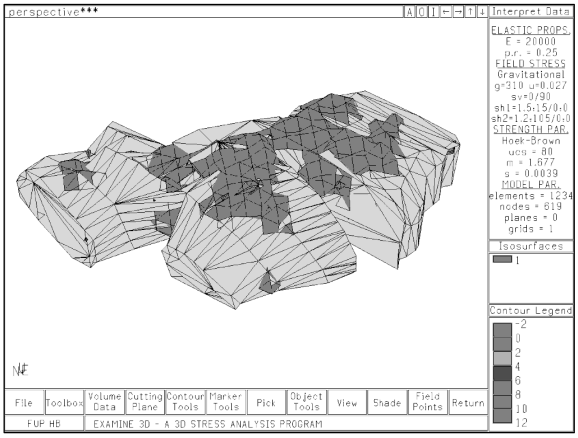

Figure 7. Isosurface for FUP=1 (Examine3D).

While the result of the contour element model was not conclusive, it was useful to highlight that the stress concentration in the roof was the main driver for instability and that local roof damage should be expected. Therefore, it was decided to produce a finite element model able to obtain a quantitative estimate of the degree of damage that could happen in the roof and to provide a factor of safety against global roof failure.

A 2D (plane strain) model was constructed with elastoplastic material behaviour. Model geometry was generated by taking a N-S cross section parallel to the pillar axis. A lithostatic vertical in-situ stress was adopted (σ_v = 4.7MPa) while horizontal stresses were calculated as per Table 2 (K_1 = 1.5), which compared reasonably to the outcome of the contour element model. Boundary conditions, mesh and geometry are shown in Figure 8.

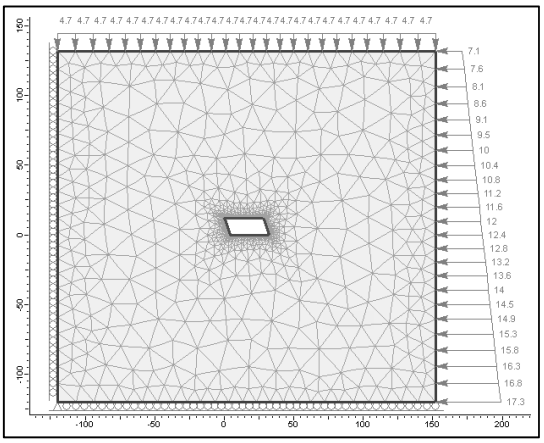

Figure 8. Boundary conditions and mesh (Phase^2).

Figure 9 shows the principal stresses distribution after the excavation and Figure 10 shows the map of maximum distortions (γ_{max} = 7‰) associated to a strength reduction factor (SRF) of 1.20. Since an admissible mechanism is developed at failure, the obtained SRF can be assimilated to an equivalent FoS. The safety factor is deemed adequate, considering that a plane strain (infinite length) model yields

conservative results when compared to a finite-length stope with stress redistribution effects that can be fully acknowledged (solely) by means of 3D modelling.

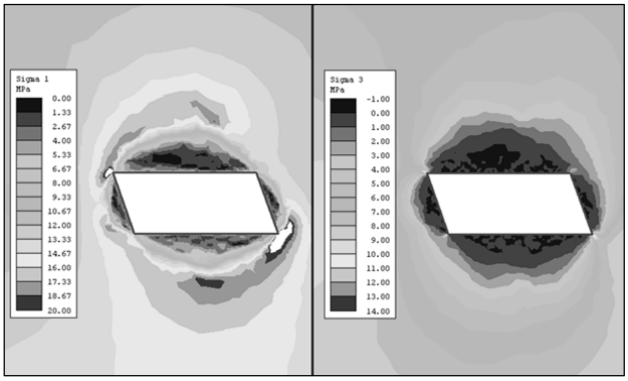

Figure 9. Distribution of principal stresses σ_1 (left) and σ_3 (right) after excavation (Phase^2).

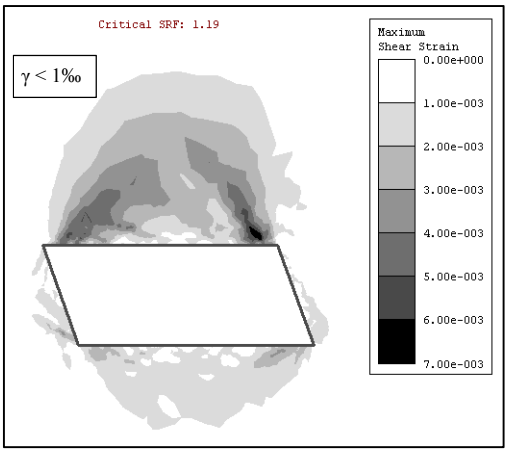

Figure 10. Maximum distortions at failure (Phase^2).

4.5 *Observed behaviour*

After blasting and mucking, the stope was surveyed with laser scanners and inspected in order to make a quick evaluation of stability conditions. The projected and as-built geometries were quite similar, with minor underbreaks ascribed to the blasting procedure. The roof underwent no sizeable overbreaks or rockfalls, thanks partly to its domed shape, and so was deemed stable. Subsequently, the stope was filled with mine waste two weeks after blasting.

5 CONCLUSIONS

Various analysis methods were employed for the stability of stopes at Arenal Deeps mine. The geological, structural and rock mass model at deposit scale were outlined, as well as the resulting parameters for the analysis set out herein. Both empirical (Potvin 1988) and numerical methods (boundary element, finite element) were employed to assess the stability of a stope roof and adjoining pillar.

Empirical procedures allowed for a straightforward determination of the need to include an intermediate pillar. The stability number yielded a value N' = 5.9, hence an admissible hydraulic radius of HR_{max} = 6.8m, whereas hydraulic radii for characteristic widths of 12.5m and 27.0m were 5.2m and 9.4m, respectively.

The complex geometry of the new design implied that further stability assessments had to be carried out using numerical procedures. A 3D boundary element model yielded induced stresses in the order of 20MPa and indicated that stress concentration in the roof was the main driver for instability.

A 2D finite element model provided a factor of safety for roof failure of 1.20, which was considered adequate, given the conservative plane-strain hypothesis it entails as well as geomechanical uncertainty.

Ultimately, numerical methods combined with a detailed geomechanical characterization were used to obtain quantitative estimates of safety for underground operations, thus enhancing widely used empirical procedures and enabling further risk estimation and operative decisions. The stope behaved adequately during the two-week lapse it was open, permitting safe and efficient mucking, surveying and inspection before being filled with mine waste.

ACKNOWLEDGEMENTS

The authors gratefully acknowledge the participation of Orosur Mining Inc, as well as the permission to publish and present this work.

Herein are also credited Antonio Samaniego and William Joughin, SRK corporate consultants who acted as reviewers of this study.

REFERENCES

AMEC International Chile S.A. 2010. Informe técnico: *Revisión y Caracterización Geotécnica y Geomecánica Preliminar para Soporte del Proyecto Mina Arenal Subterránea.*

Hoek E., Carranza-Torres C.T., Corkum B. 2002. Hoek-Brown failure criterion-2002 edition. *Proceedings of the fifth North American rock mechanics symposium* 1: 267–273.

Hoek, E., and Diederichs, M.S. 2006. Empirical estimation of rock mass modulus. *International Journal of Rock Mechanics and Mining Sciences*, 43: 203–215.

Mello J., González L. G., Carrasco F. 2010. *Revisión y caracterización geotécnica y geomecánica preliminar para soporte del proyecto mina Arenal subterránea*. AMEC International.

Nickson, S. D. 1992. *Cablebolt support guidelines for underground hard rock mine operations*. MASc thesis (unpublished), University of British Columbia, Vancouver, British Columbia, Canada.

Orosur Mining Inc 2010. *Proyecto Arenal Subterráneo, Asunto 69/2004, Tomo I.*

Potvin, Y. 1988. *Empirical open-stope design in Canada*. PhD thesis, University of British Columbia, Vancouver, British Columbia, Canada, 350.

Villaescusa, E. 2014. *Geotechnical design for sublevel open stoping*. CRC Press.